Biogeosciences

Effects of cyanobacterial-driven pH increases on sediment nutrient fluxes and coupled nitrification-denitrification in a shallow fresh water estuary

Y. Gao, J. C. Cornwell, D. K. Stoecker, and M. S. Owens

Horn Point Laboratory, University of Maryland Center for Environmental Science, P.O. Box 775, Cambridge, MD, USA

Correspondence to: J. Cornwell (cornwell@umces.edu)

Abstract. Summer cyanobacterial blooms caused an elevation in pH (9 to $\sim$10.5) that lasted for weeks in the shallow and tidal-fresh region of the Sassafras River, a tributary of Chesapeake Bay (USA). Elevated pH promoted desorption of sedimentary inorganic phosphorus and facilitated conversion of ammonium (NH_4^+) to ammonia (NH_3). In this study, we investigated pH effects on exchangeable NH_4^+ desorption, pore water diffusion and the flux rates of NH_4^+, soluble reactive phosphorus (SRP) and nitrate (NO_3^-), nitrification, denitrification, and oxygen consumption. Elevated pH enhanced desorption of exchangeable NH_4^+ through NH_3 formation from both pore water and adsorbed NH_4^+ pools. Progressive penetration of high pH from the overlying water into sediment promoted the mobility of SRP and the release of total ammonium (NH_4^+ and NH_3) into the pore water. At elevated pH levels, high sediment-water effluxes of SRP and total ammonium were associated with reduction of nitrification, denitrification and oxygen consumption rates. Alkaline pH and the toxicity of NH_3 may inhibit nitrification in the thin aerobic zone, simultaneously constraining coupled nitrification–denitrification with limited NO_3^- supply and high pH penetration into the anaerobic zone. Geochemical feedbacks to pH elevation, such as enhancement of dissolved nutrient effluxes and reduction in N_2 loss via denitrification, may enhance the persistence of cyanobacterial blooms in shallow water ecosystems.

1 Introduction

Nutrient releases from sediment into the water column can support a substantial fraction of the primary production in shallow coastal and estuarine ecosystems (e.g. North Carolina estuaries, Fisher et al., 1982; Potomac River Estuary, Kemp and Boynton, 1984; Baltic Sea, Koop et al., 1990; Chesapeake Bay, Cowan and Boynton, 1996). Enhanced nitrogen and phosphorus fluxes may promote high levels of phytoplankton biomass (Kemp et al., 2005). Such phytoplankton blooms lead to the sustained accumulation of phytodetritus in sediment, fueling nutrient recycling through organic matter remineralization (Cowan and Boynton, 1996; Nixon et al., 1996). The consequences, such as decreased water clarity, depletion of bottom-water oxygen and the decomposition of phytodetritus, may enhance sediment respiration, decrease redox potential, limit nutrient uptake by benthic microalgae, and generally increase nutrient fluxes (Kemp et al., 2005).

In the deep, anoxic region of the Chesapeake Bay and other estuaries, phosphorus flux is usually promoted by the dissolution of Fe-oxides and their conversion to iron sulfides (Cornwell and Sampou, 1995; Roden and Tuttle, 1992). The increase in ammonium release from sediments tends to coincide with inhibition of nitrification by oxygen depletion and generation of reductants (HS^-/H_2S) in sediment, which consequently constrain denitrification (Kemp et al., 2005; Cornwell et al., 1999). Nevertheless, in oxic shallow water ecosystems, benthic nutrient releases are generally less redox influenced.

Driven by rapid utilization rates of inorganic carbon for photosynthesis during dense algal blooms (Hansen, 2002;

Hinga, 2002), persistent high pH in shallow water can influence benthic dynamics with progressive pH penetration from the overlying water into sediments (Bailey et al., 2006). When pH is above a critical threshold (9–9.2), inorganic phosphorus desorbs from iron oxides at mineral surfaces (Andersen, 1975; Eckert et al., 1997). Elevation of pore water pH ($\sim$9.8 in tidal-fresh regions, Eckert et al., 1997) can promote sediment release of soluble reactive phosphorus (SRP), and simultaneously support P demand during cyanobacterial blooms in lakes (Xie et al., 2003) and tidal fresh and oligohaline estuaries (Seitzinger, 1991; Andersen, 1975).

In contrast to pH-driven P cycling, the effects of pH on sediment N transformations and release are not well understood (Soetaert et al., 2007). During the decomposition of sediment organic matter, remineralized ammonium (NH_4^+) may both adsorb onto sediment mineral surfaces and accumulate in pore water. Exchangeable NH_4^+ is weakly bonded to negatively charged particle surfaces, buffering pore water NH_4^+ concentrations (Rosenfeld, 1979). In estuaries, fine grained sediment generally has a large pool of adsorbed NH_4^+ (Wang and Alva, 2000; Weston et al., 2010), with freshwater sediments having considerably more adsorbed ammonium relative to saline sediments (Seitzinger, 1991). Once alkaline pH results in the conversion of NH_4^+ to dissolved ammonia (NH_3), formation of non-ionized NH_3 may decrease NH_4^+ cation adsorption on sediments and potentially alter the balance between pore water and exchangeable NH_4^+.

Besides assimilation by plants and bacteria, remineralized N can diffuse/advect from sediment into the overlying water. Alternatively, part of the NH_4^+ can be oxidized sequentially to NO_2^-/NO_3^- and then reduced to N_2 in the suboxic/anoxic layer (Cornwell et al., 1999). However, shifts in the NH_4^+-NH_3 equilibrium, associated with high pH penetration passing through the redox boundary, may change the rates of pore water diffusion and nitrification-denitrification. In the tidal-fresh and oligohaline parts of the Potomac River (Chesapeake Bay), Seitzinger (1987) observed both increased SRP and NH_4^+ fluxes with pH elevation. Experimental NH_4^+ flux rates increased from <10 to over $100\,\mu\mathrm{mol}\,\mathrm{m}^{-2}\,\mathrm{h}^{-1}$ when pH was raised from 8 to 10 in laboratory incubations (Seitzinger, 1987). During an algal bloom in the Potomac estuary, Bailey et al. (2006) observed a three-fold increase of NH_4^+ efflux when the bottom water pH rose from neutral to above 9. In soil studies, the combined influence of alkaline pH (>8) and toxic NH_3 production can reduce the NH_4^+ soil inventory due to NH_3 volatilization, decrease the efficiency of nitrification and denitrification, and inhibit enzyme activity as well (Simek et al., 2002; Cuhel et al., 2010).

We hypothesize that increased sediment pH facilitates not only P desorption but also the conversion of NH_4^+ to NH_3 with consequent changes in sediment N cycling. In this study we examined the influence of pH on exchangeable NH_4^+ desorption in near-surface sediments. Impacts of high pH condition on sediment-water nutrient exchange were de-

termined via flux rate measurements of dissolved nutrients (SRP, NH_4^+, NO_3^-), respiration rates (O_2), and denitrification rates (N_2) using intact sediment cores. We also calculated the diffusive flux rates of pore water NH_4^+, NH_3 and SRP to confirm direct flux measurements.

Since nitrification products may be released as NO_3^- and denitrified, we independently measured potential nitrification rates using slurries (Henriksen et al., 1981) and nitrification rates using an inhibitor (Caffrey and Miller, 1995). The potential nitrification method makes testing pH effects over a large pH gradient relatively simple, although it homogenizes the vertical gradients in sediments (e.g. redox potential and NH_4^+) and disrupts the aggregation of aerobic/anaerobic microbiota (Killham, 1994; Garcia-Ruiz et al., 1998). A CH_3F-inhibition method can make up the shortcomings of slurry experiments. The shortcoming of nitrifying inhibitor likely leads to increased accumulation of pore water ammonium and non-specific inhibition of other N transformations such as ammonification (Capone et al., 2009). Therefore, both methods were taken to compare the nitrification responses to pH elevation.

We experimentally addressed these questions using sediment cores incubated with a continuous water flow-through system. In the Chesapeake Bay, cyanobacterial blooms occur frequently in the shallow and tidal freshwater tributaries, such as the Sassafras River and Potomac River (Tango and Butler, 2008). Relative to sea water, tidal fresh and oligohaline water have low pH buffering (Price et al., 2008), facilitating high pH levels from cyanobacterial photosynthetic carbon uptake. During dense cyanobacterial blooms at the Sassafras River, high pH persisted in the range of 9 to 10.5 for several weeks (eyesonthebay.net). When such high pH is in contact with bottom sediment, pH penetration into sediment can impact nutrient biogeochemical processes (Bailey et al., 2006).

2   Materials and methods

2.1   Study site and collection of cores

In the upper Sassafras River, we collected sediments at the Powerline site (75°49.712′, 39°22.646′) on 18 June 2008 and Budds Landing (75°50.380′, 39°22.310′) on 14 July 2009 using 7 cm-inner diameter, 30 cm-long acrylic cores (Table 1). Water depths were 0.8 m at Powerline and 1.3 m at Budds Landing. Dissolved oxygen (DO), salinity, pH and temperature were measured with a YSI 600XLM multiparameter sensor. Vertical profiles of irradiance were recorded using a 2π Li-Cor underwater PAR light sensor. Bottom water was pumped through an inline filter (nominally 0.8 μM) to minimize autotrophic and microbial respiration, and nutrient recycling as well. We transported samples to Horn Point Laboratory within 4 h. Sediment cores were gently aerated overnight with aquarium pumps in order to reach oxygen

Table 1. Sediment grain size, ambient dissolved nutrients in water column and the flux rates before pH modification. Samples were collected at the Powerline site on 18 June 2008 and Budds Landing site on 14 July 2009. Grain size measurements were made after flux experiments; other measurements for dissolved nutrient concentrations (average $\pm$ SE, $n = 3$) in the bottom water and flux rates (mean $\pm$ SE, $n = 4$–9) were carried out before pH treatments. Negative flux rates indicate uptake by the sediment.

Variables	Powerline	Budds Landing
Grain size (%)		
sand	3.2	6.7
silt	59.9	58.8
clay	36.9	34.4
Bottom water characterization		
SRP (μmol l^{-1})	0.7 ± 0.04	0.23 ± 0.07
NH$_4^+$ (μmol l^{-1})	2.1 ± 0.05	0.6 ± 0.1
NO$_3^-$ (μmol l^{-1})	7.5 ± 0.02	0.82 ± 0.02
Salinity	0.05	0.2
Temperature ($^\circ$C)	24.7	26.9
pH	9.4	7.3
DO (mg l^{-1})	10.3	12.48
Chl a (μg l^{-1})	78	46.5
Core fluxes (μmol m^{-2} h^{-1})		
SRP flux	-0.2 ± 1.2	5.0 ± 3.7
NH$_4^+$ flux	62 ± 8.5	310 ± 32
NO$_3^-$ flux	-41 ± 0.2	10 ± 18
N$_2$ flux rate	259 ± 38	176 ± 21
O$_2$ flux rate	-1614 ± 62	-2240 ± 193

Table 2. Experimental overlying water pHs for experimental incubation of cores from the Powerline and Budds Landing sites. The Powerline incubations had a sequential change of pH ($n = 4$). The Budds Landing incubation had all cores ($n = 9$) at neutral pH on the first day, and then set 3 replicate cores at 3 different pHs, respectively. pH data are the mean values $\pm$ SE.

Treatments	Powerline		Budds Landing	
	Time (day)	pH	Time (day)	pH
Control	1st	7.8 ± 0.01	1st and 7th	7.4 ± 0.3
pH_mid	6th	9.2 ± 0.02	7th	9.2 ± 0.05
pH_high	11th	9.6 ± 0.03	7th	9.5 ± 0.2

saturation before experimentation and to equilibrate temperature, O$_2$, and N$_2$-N in the overlying water and near surface pore waters (Kana et al., 2006). Although photosynthetic carbon removal may result in high in situ pH (Table 1), the experimental aeration increased the dissolved CO$_2$ concentration and pH neutralization in the water column (Table 2). Surface sediments (top 2 cm) were homogenized for potential nitrification measurements, while the remaining sediment core was used for grain size measurement.

2.2 Experimental design

We incubated experimental cores (at least triplicates) at several pH levels to investigate pH effects on nutrient exchange at the sediment-water interface. Sediment-free blank cores were incubated identically at each pH level to correct for water column metabolic activity and nutrient cycling. Consistent with an absence of photosynthetically active radiation in bottom water at the time of collection, a dark temperature-controlled environmental chamber was used to maintain the sediments and replacement-water reservoir at in situ water temperatures of 25 $^\circ$C for Powerline and 27 $^\circ$C

for Budds Landing, respectively. Sediment cores were sealed with acrylic o-ring tops that suspended a magnetic stir-bar beneath it, and a rotating magnetic turntable was set in the center that drove all magnetic bars to mix the overlying water at same speed. A flow-through system was set up for each core, which faciliated maintaining constant conditions (e.g. pH, nutrient levels, oxygen, flow speed) inside of sediment cores. In each water reservoir, the filtered water was bubbled with air to maintain saturated oxygen and adjusted to the desired pH with 0.1 mol l^{-1} NaOH. We continuously pumped water from reservoirs into the overlying water ($\sim$500 ml) of the cores at 10 ml min^{-1} using a Rainin Rabbit peristaltic pump.

For the Powerline experiments, the overlying water pH of 4 replicate sediment cores was increased stepwise from 7.8 ± 0.5 to 9.2 ± 0.05 and 9.6 ± 0.03, with a five-day equilibration at each elevated pH. An alternative approach was used with sediments from Budds Landing. Nine cores were incubated at ambient pH for the initial fluxes, and then triplicate cores were subjected to pH manipulation for each treatment. After 7 days of exposure to higher pH levels, the overlying water pHs were 7.4 ± 0.3, 9.2 ± 0.05, and 9.5 ± 0.2 (Table 2).

For both sites, nutrient fluxes (SRP, NH$_4^+$ and NO$_3^-$), oxygen consumption (O$_2$) and coupled nitrification–denitrification (net N$_2$ flux) were measured on the 1st day of incubation of sediments and after the pH reached the target values. After the termination of flux incubations, the sediments from each pH treatment were sectioned for pore water profiles of nutrients and determination of pH. Sediment cores from Budds Landing were used to evaluate the pH impacts on nitrification rates and ammonium desorption. Based on Br$^-$ penetration (Martin and Banta, 1992), we estimated the diffusion/advection coefficients of NH$_4^+$, NH$_3^+$ and SRP. The remaining sediment cores were used to estimate the percent water content.

2.3 Flux rates cross the sediment-water interface

Flux rates were measured on the first day of the incubation and after each equilibration period. The pumping of

treatment water was interrupted during flux measurements and briefly restarted to collect samples every 1.5 h, with a total of 4 time-points. Solute samples were filtered through a 0.45 μm cellulose acetate syringe filter and frozen at $-4\,^\circ\mathrm{C}$. Dissolved O_2 and N_2 subsamples were preserved in 7 ml glass tubes by adding 10 μl of 50 % saturated $HgCl_2$ solution (Kana et al., 2006), and stored under water at near-ambient temperature until analysis. To preserve total dissolved ammonium ($\sum NH_x = NH_4^+ + NH_3$) at higher pH levels, 2.5 μl of $0.1\,\mathrm{mol\,l^{-1}}$ sulfuric acid was added into the sample vials. Flux rates were calculated from the regression coefficients of the time-concentration data in sediment. Blank incubations were used to correct sediment core fluxes for any changes in concentration caused by water column activity.

2.4 Sediment pore-water chemistry

Over the top $\sim$10 cm sediments, samples were sectioned for pH and pore water analysis in a nitrogen-filled glove bag to minimize oxidation artifacts (Bray et al., 1973). Vertical changes of pH were measured immediately with a flat surface pH electrode. Sediments were sectioned into 50 ml centrifuge tubes and centrifuged at 2000 G for 10 min. Supernatant solutions were filtered through a 0.45 μm 25 mm diameter cellulose acetate syringe filter and appropriately diluted for analysis of Br^-, Fe, SRP, NH_4^+, and $\sum NH_x$. The total iron, mostly Fe^{2+}, was acidified for preservation (Gibbs, 1979).

2.5 Nitrification potential and nitrification rates

The effect of pH on nitrification was estimated using sediments from Budds Landing. Measurements included slurry incubation for potential nitrification (Henriksen et al., 1981) and CH_3F inhibition of nitrification in intact sediment cores (Caffrey and Miller, 1995). Potential nitrification was measured with the surface sediments (0–2 cm depth) from Budds Landing. In O_2-saturated Sassafras River water, pH was pre-adjusted with NaOH to values from 7 to 11. For 3 centrifuge tubes at each pH level, we added NH_4Cl to final concentration of 1.0 mM and then added 1ml homogenized sediment. We gently mixed the suspensions in darkness at $27\,^\circ\mathrm{C}$ using a orbital shaker, and took subsamples for NO_3^- at 0, 12, and 24 h to calculate rates of potential nitrification. Changes of NO_3^- in a sediment-free control were used as a background correction.

Alternatively, nitrification rates were measured based on the assumption that addition of CH_3F can cut off nitrification and enhance direct NH_4^+ fluxes (Caffrey and Miller, 1995). The CH_3F method was carried out immediately after the end of flux measurements. Briefly, saturated solutions of CH_3F were injected into the overlying water of intact cores to a final concentration of $\sim$100 mg l^{-1}. After 24 h of aerobic dark pre-incubation, ammonium flux rates were measured using our standard flux procedure. Due to the inhibition of am-

monium oxidation, increased flux rates of ammonium after CH_3F treatment were interpreted as the nitrification rate.

2.6 Molecular diffusive flux rates

Diffusion coefficients in sediment were estimated from Br^- penetration profiles (Martin and Banta, 1992). Bromide (NaBr) was added as a tracer into the overlying water to a final concentration of $\sim$6 mM. After 24 h, vertical profiles of pore water Br^- were measured to calculate the diffusion coefficient (D_{Br}), which was corrected for temperature and sediment porosity. The measured D_{Br} was compared to the theoretical coefficient (D_{Br}^*) to aid in correction of diffusion coefficients for other species (Martin and Banta, 1992; Schulz et al., 2006; Rao and Jahnke, 2004).

Using the pH-dependent equilibrium (Eq. 1), we calculated pore water NH_3 and NH_4^+ concentrations:

$$NH_4^+ + OH^- \underset{}{\overset{K_a}{\rightleftharpoons}} NH_3 + H_2O, \tag{1}$$

where the equilibrium constant (pK_a) is 9.25 at 25 °C; constants were corrected for ionic strength and temperature (Mulholland, 2008).

The dissolved NH_3 concentration, $[NH_3]$, can be calculated (Van Nester and Duce, 1987):

$$[NH_3] = \frac{[\sum NH_x][OH^-]}{K_b + [OH^-]}, \tag{2}$$

where $[\sum NH_x]$ is the sum of dissolved NH_3 and NH_4^+.

The diffusion coefficients (D_i) of NH_3, NH_4^+ and SRP were corrected using the Br^- diffusion estimates in pore water and the theoretical coefficient (D_{Br}^*). Applying Fick's first law, the NH_3, NH_4^+ and SRP fluxes were calculated by:

$$F_i = -\emptyset \cdot D_i \times \frac{\partial C_i}{\partial x}, \tag{3}$$

where F_i is the flux of different species (μmol cm^{-2} s^{-1}). The diffusion coefficient (D_i) is influenced by tortuosity (θ), temperature and sediment properties; $\frac{\partial C_i}{\partial x}$ is the gradient of nutrient concentration (C_i) and depth (x) (Table 3). The diffusion coefficients of NH_3, NH_4^+ and SRP in sediments were corrected using the D_{Br} estimates and the diffusion coefficients in a particle free solution at in situ temperature (Martin and Banta, 1992; Rao and Jahnke, 2004; Schulz et al., 2006). Percent water and the dry sediment density ($\rho \sim$2.5 g cm^{-3}) were used to calculate porosity ($\emptyset$) (Boudreau, 1997):

$$\emptyset = \frac{\text{water\%}}{(\text{water\%} + \frac{(1 - \text{water\%})}{\rho.})} \tag{4}$$

2.7 Desorption isotherm of adsorbed ammonium (NH_4^+-N)

In order to estimate pH effects on ammonium desorption from sediment, surface sediments were collected from Budds

Table 3. The kinetic parameters used in calculation of diffusion rates and in calculation of ammonium adsorption-desorption in sediments.

Parameter	Value	Comments	Ref.
pK_b	4.75	$pK_b = 14 - pK_a$	
Temperature	27.0 °C		
For calculation of the molecular diffusive rates			Stumm and Morgan (1996)
water %	74 %	10 cm	
ρ	2.50	g cm^{-3}	
$\varnothing$	0.88		
θ^2	1.26		
D*-Br$^-$	20.10	The diffusion coefficient in free	Li and Gregory (1974)
D*-PO$_4^{3-}$	5.77	solution (D*: 10^{-6} cm^2 s^{-1})	
D*-NH$_4^+$	19.80		
D*-NH$_3$	24.52		
D-KBr$^-$	1.09	The corrected diffusion coefficient	
D-SRP	0.30	(D: 10^{-6} cm s^{-1})	
D-NH$_4^+$	1.02		
D-NH$_3$	1.29		
For adsorption coefficient of ammonium at top 2 cm sediment			
water %	89 %	top 2 cm	
$\varnothing$	0.95	top 2 cm	
$\hat{C}_N$	1.5 ± 0.2	µmol g^{-1} wet sediment	
C_N	0.07	µmol ml^{-1}	
For ammonium desorption			
R	8.2×10^{-5}	atom m^3 mol^{-1} K^{-1}	Larsen et al. (2001)
H-NH$_3$	7.05×10^{-2}	mol atm^{-1} m^{-3}	Capone et al. (2009)
H's-NH$_3$	1.72×10^{-3}		
I	1.47×10^{-3}		
γ_{NH_3}	1.00		
$\gamma_{NH_4^+}$	0.88		

Landing in November 2008. Adsorbed NH$_4^+$ was measured using KCl extraction (Morin and Morse, 1999). Triplicate 1 ml wet samples of the top 2 cm sediment were extracted twice with 39 ml of 2 mol l^{-1} KCl; samples were shaken for 2 h at the field temperature (10 °C). After centrifugation and filtration, the increase in NH$_4^+$ concentration relative to the blank was used to quantify adsorbed ammonium. Adsorption coefficients (K) were used to describe this ion exchange behavior, following Rosenfeld (1979) and Mackin and Aller (1984):

$$K = \rho \cdot \frac{1 - \varnothing}{\varnothing} \cdot \frac{\hat{C}_N}{C_N} \quad (5)$$

where $\hat{C}_N$ is exchangeable NH$_4^+$ on a dry mass basis (µmol g^{-1}) and C_N is the pore water ammonium concentration (µmol l^{-1}). Porosity was measured for the top 2 cm of sediment (Table 3).

To simulate response of adsorbed ammonium to pH elevation, the homogenized sediment (0–2 cm) was suspended in pH adjusted water from the sampling site. We added 1 ml of wet sediment to 39 ml of pH-adjusted water. To inhibit dissimilatory NO$_3^-$ reduction to NH$_4^+$, we used oxygen-saturated water and left 5 ml headspace in the centrifuge tube. $\sum$NH$_x$ was measured after shaking, centrifugation and filtration. Assuming a NH$_3$ equilibrium between the aquatic and atmospheric phase, the total release of ammonium is estimated as the sum of total dissolved ammonium in the sample water (ΣNH$_{x,l}$) and NH$_3$ gas within the head space (NH$_{3-g}$):

$$NH_{x_{ds}} = \Delta \Sigma NH_{x,l} + \Delta NH_{3-g} \quad (6)$$

The headspace NH$_3$ was estimated from (1) the pH at the end of incubation, (2) ionic strength corrections for NH$_3$ (γ_{NH_3}) and NH$_4^+$ ($\gamma_{NH_4^+}$), and (3) the temperature-corrected Henry's law coefficient ($H'_s = RTH$) (Larsen et al., 2001):

$$[NH_3] = \frac{[\Sigma NH_x]}{RTH \left(\frac{1}{\gamma_{NH_3}} + \frac{10^{-pH}}{K_a \gamma_{NH_4^+}} \right)} \quad (7)$$

2.8 Chemical analysis

Concentrations of NH_4^+, SRP and Fe were analyzed using colorimetric methods (Gibbs, 1979; Parsons et al., 1984). Concentrations of NO_3^-, NO_2^- and pore water Br^- were determined using ion chromatography (Kopp and McKee, 1983). Dissolved N_2 and O_2 were measured by the ratios of N_2:Ar and O_2:Ar using membrane inlet mass spectrometry (Kana and Weiss, 2004; Kana et al., 1994). Percent water was determined as the weight loss of wet sediment after drying at $65\,^\circ$C. After pre-treatment with sodium hypochlorite overnight to remove carbonates and organic matter, grain size was analyzed by wet sieving and followed by pipet analysis of the remaining silt and clay (Folk, 1974).

3 Results and discussion

3.1 Physical conditions

The Powerline and Budds Landing sites have similar physical conditions, including shallow and aerobic water columns, low salinity (<0.2), and fine grain-sized sediments (Table 1). Light attenuation coefficients were $4.8\,\mathrm{m}^{-1}$ at Powerline and $4.2\,\mathrm{m}^{-1}$ at Budds Landing, resulting in dim to dark conditions at the sediment surface. Both sites often have experienced cyanobacterial blooms associated with high pH in summer (Maryland Department of Natural Resources, eyesonthebay.net). At the time of collection, in situ pH was 9.4 and 7.3 in bottom water at Powerline and Budds Landing, respectively (Table 1). After the air-water DIC equilibrium overnight, the initial pH levels were neutral and similar in our experimental control groups (Table 2).

3.2 Penetration of pH and pore water iron

Vertical profiles of pH and Fe rapidly responded to the diffusion of overlying water pH ($=9.6$) into the pore water (Fig. 1a and b). Sediment pH under ambient condition indicated a weak acid condition, being nearly constant with depth; the elevated pH water column treatments resulted in pH > 9.0 in the top 1–2 cm of sediment, decreasing downward until values were similar to the control. Although pH may be buffered by cation exchange (e.g. Ca^{2+}, Mg^{2+}), sulfate reduction, and anaerobic generation of acid (Cai et al., 2010), such high pore water pH levels (pH > 9.5) have been observed during algal blooms in tidal-freshwater estuaries (Magalhaes et al., 2002). Our elevated pH profiles in sediments were similar to a time-series study of pH penetration by Bailey et al. (2006) in the Potomac River. Sediment incubations at high pH ($\sim$10) showed a downward movement of high pH over time and achieved pH > 9 at 4 to 8 cm depth in a week incubation (Bailey et al., 2006).

In our aerobic incubations, pore water Fe^{2+} was undetectable at the surface and peaked in the upper anoxic sediment horizon. Increased pH lead to a reduction in Fe^{2+}
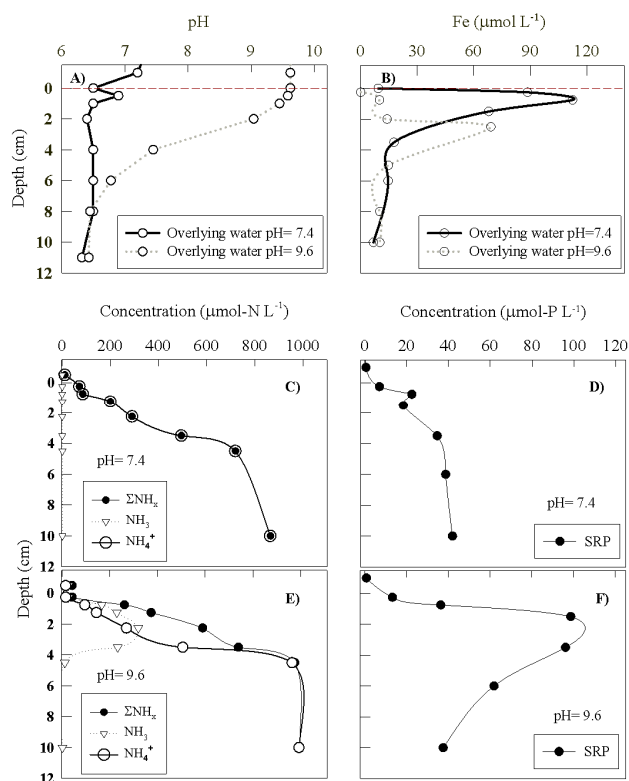

Fig. 1. Powerline pore water profiles in the upper 10 cm of sediment under high pH (9.6) and normal pH (7.4) treatments, including vertical changes of pH (**A**), pore water Fe (**B**), SRP (**D, F**), and $\sum NH_x$ (**C, E**). The dashed line is the interface of sediment-water. Changes in ammonium speciation, resulted from surface pH elevation, were calculated by the equilibrium of NH_3 and NH_4^+.

through hydroxide precipitation (Hutchins et al., 2007). As pH increased to 9.6 in the overlying water, the peak concentration of Fe^{2+} simultaneously decreased from $118\,\mu\mathrm{mol\,l}^{-1}$ to $64\,\mu\mathrm{mol\,l}^{-1}$, and its peak position shifted from 1.75 cm downward to 2.5 cm.

3.3 Effect of pH on the pore water SRP profile

Elevation of pH below the sediment-water interface to P release into pore water, with the peak SRP concentrations increasing from $<40\,\mu\mathrm{mol\,l}^{-1}$ to $102\,\mu\mathrm{mol\,l}^{-1}$ (Fig. 1d and f). This change was consistent with pH-related P releases from surface metal hydroxide complexes (Seitzinger, 1991; Boers, 1991). Under aerobic pH-neutral conditions, iron oxyhydroxides usually adsorb or co-precipitate P, hindering the flux of SRP across the sediment-water interface (Slomp et al., 1998). In contrast to neutral pH conditions, highly alkaline pH levels enhanced P mobility by breaking surficial Fe-P bonds, which increased pore water SRP gradients and the diffusion rate (Figs. 1 and 2). As expected, elevated pH increased upward SRP diffusion from $5\,\mu\mathrm{mol\,m}^{-2}\,\mathrm{h}^{-1}$ under
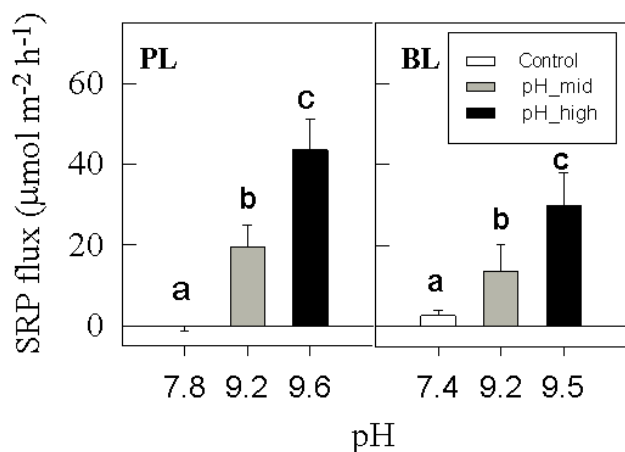
Fig. 2. Experimental pH effects on SRP flux rates from sediments at Powerline (PL) and Budds Landing (BL). Error bars are the standard errors. Two-way ANOVA was used to test the pH effects on SRP release at both sites. With elevation in the experimental pH, SRP fluxes were significantly different at each site ($P < 0.01$), but nonsignificantly different between stations ($P > 0.05$). Different letters are used to show significant difference.

neutral pH to $39 \, \mu\text{mol m}^{-2} \, \text{h}^{-1}$ under alkaline pH treatments (Fig. 1 and Tables 3, 4).

3.4 Effect of pH on SRP flux

Flux rates of SRP significantly increased as pH increased at both stations (Fig. 2). SRP efflux rates increased from $< 5 \, \mu\text{mol m}^{-2} \, \text{h}^{-1}$ in the control, to 15–$25 \, \mu\text{mol m}^{-2} \, \text{h}^{-1}$ at pH 9.2, and to 35–$55 \, \mu\text{mol m}^{-2} \, \text{h}^{-1}$ at pH 9.6 (Fig. 2). SRP release at the Powerline site were consistent with its molecular diffusive rates estimated from pore water profiles (Table 4). In the oligohaline region of the Potomac River, SRP release from sediment increased from $< 10 \, \mu\text{mol m}^{-2} \, \text{h}^{-1}$ at neutral controls, to $\sim 40 \, \mu\text{mol m}^{-2} \, \text{h}^{-1}$ at pH 9.5, and to $\sim 110 \, \mu\text{mol m}^{-2} \, \text{h}^{-1}$ at pH 10 (Seitzinger, 1991). Similar large increases in SRP flux rates have been observed at pH levels of 9.5 in freshwater sediments (Boers, 1991).

3.5 Adsorbed NH_4^+

Adsorbed NH_4^+ is reversibly attracted to negatively charged binding sites on the surface of sediment particles (Rosenfeld, 1979), and can influence pore water NH_4^+ concentration as well as migration within sediment (Morse and Morin, 2005). Both pore water and adsorbed ammonium are hypothesized to be available for nitrification (Seitzinger et al., 1991). Without pH manipulation, adsorbed NH_4^+ in our samples averaged $3400 \pm 400 \, \text{nmol g}^{-1}$-dry sediment (Fig. 3). It is reasonable to expect higher adsorbed NH_4^+ in summer due to spring/summer algal deposition and the temperature-related increases in ammonification (Laima et al., 1999; Laima, 1992; Vouve et al., 2000). Our adsorption coefficient

$(K = 2.6 \pm 0.4)$ were similar to the observations of 2.1–7.1 in Potomac River sediments (Simon and Kennedy, 1987) and in the upper Chesapeake Bay (Cornwell and Owens, 2011). The K value in this freshwater estuary is higher than other coastal sediments (1.0–1.7, Mackin and Aller, 1984) and marine sediments (1.1–1.3, Rosenfeld, 1979), which may result from different salinity influences on NH_4^+ adsorption (Seitzinger et al., 1991b; Weston et al., 2010).

3.6 Effect of pH on desorption of sediment NH_4^+

Calculated from $\sum NH_x$ and pH changes in water, the peak of dissolved NH_4^+ was $132 \, \mu\text{mol l}^{-1}$ at pH 8.9 while NH_3 gradually increased with pH from the upper 8s (Fig. 3a). Desorbed NH_4^+ increased from 646 to $2647 \, \text{nmol g}^{-1}$ as pH rose from 6.5 to 12 (Fig. 3b). Increased pH stimulated the release of the absorbed ammonium into pore water via the conversion of NH_4^+ to NH_3. Although mineral surface charges become more and more negative as pH increased, un-ionized NH_3 did not substantially adsorb to the solid phase. At pH < 8.9, both increases in NH_4^+ and NH_3 (Fig. 3a) likely resulted from the desorption of exchangeable NH_4^+ from mineral surface. When pH approached pK_a (i.e. pH $= 9.25$), NH_4^+ conversion rate ($-\Delta NH_4^+ / \Delta pH$) peaked with 53 % of ammonium ($\sum NH_x$) converted into NH_3 (Eq. 2). Moreover, a positive relationship existed between the absorbed NH_4^+ on mineral surfaces and NH_4^+ concentrations in the pore water (Eq. 5). Elevated pH (~ 9 to 12) lead to a sharp decrease in NH_4^+ in the pore water (Fig. 3a) and more than 90 % of ammonium was transformed to NH_3. The loss of NH_4^+, along with un-ionized NH_3 formation, may further mobilize absorbed ammonium until approximately 80 % of exchangeable ammonium was desorbed (Fig. 3b).

3.7 Effect of pH on the pore water ammonium profile

Under normal pH conditions, NH_4^+ linearly increased downcore to $720 \, \mu\text{mol l}^{-1}$ with negligible NH_3 present (Fig. 1c). The diffusive flux rate, primarily as NH_4^+, was $149 \, \mu\text{mol m}^{-2} \, \text{h}^{-1}$ (Table 4). In contrast, the $\sum NH_x$ concentration in the pH 9.6 treatment increased to $975 \, \mu\text{mol l}^{-1}$ at ~ 3 cm depth (Fig. 1e), reflecting pH-driven ammonium desorption from solid phase to pore water. Relative to $\sum NH_x$ profile, conversion of NH_4^+ to NH_3 in surface horizons resulted in a steeper concentration gradient of NH_4^+, increasing NH_4^+ diffusive fluxes (Table 4). Similar to observations of salinity-enhanced ammonium desorption (Gardner et al., 1991), reduction in NH_4^+ concentrations at surface may further promote ammonium desorption (Eq. 5). Dissolved NH_3 exhibited a very sharp peak at 0–3 cm depth, yielding a rapid upward flux. Diffusive flux rates were the sum of $243 \, \mu\text{mol m}^{-2} \, \text{h}^{-1}$ for NH_4^+ and $234 \, \mu\text{mol m}^{-2} \, \text{h}^{-1}$ for NH_3 (Table 4). Without consideration of $\sum NH_x$ speciation in high pH cores, the diffusive rate calculated from the concentration gradient and diffusion coefficient of NH_4^+

Table 4. Efflux rates of SRP and $\sum NH_x$ in control and in high pH treatments in sediment cores from Powerline. Net flux rates ($\pm SE$) were compared to rates estimated from molecular diffusion of pore water.

Treatment	The overlying water pH	SRP flux rates (μmol-P m^2 h^{-1})		Ammonium flux rates (μmol-N m^2 h^{-1})			
		Diffusive rate	Flux rate	Diffusive rate			Flux rate
				NH_4^+	NH_3	$\sum NH_x$	$\sum NH_x$
Control	7.8 ± 0.01	4.6	3 ± 3.2	149.5	0.2	149.7	61.7 ± 8.5
High pH	9.6 ± 0.03	39.2	43.5 ± 7.4	243.1	234.2	477.3	440.9 ± 19.1

was only $271\,\mu mol\,m^{-2}\,h^{-1}$, less than half of the observed $\sum NH_x$ diffusive rate (Fig. 1e).

3.8 Effect of pH on DIN flux

For both Powerline and Budds Landing experimental cores (Fig. 4a), flux rates of $\sum NH_x$ increased significantly in the high pH treatments relative to the control ($p < 0.05$, two-way ANOVA), but differences between pH 9.2 and 9.5 were not always significant. Compared to the control group, high pH (9.5–9.6) promoted $\sum NH_x$ flux rates by about 6-fold at Powerline and by 2-fold at Budds Landing. These increases were consistent with the pH-induced ammonium desorption at surface sediments and the observed changes in the pore water profile. The conversion of NH_4^+ to NH_3 and the steeper concentration gradients of these two components all resulted in elevated $\sum NH_x$ fluxes. At the Powerline site, the ammonium release in the control was similar to the upward diffusion rate of ammonium, primarily as NH_4^+. The measured efflux rates of $\sum NH_x$ at pH 9.6 were equivalent to the sum of the diffusive flux rate of NH_4^+ and NH_3 (Table 4). Lack of consideration of NH_3 production would result in underestimation of ammonium flux rates by 25–35 % for the flux measurement and by 50 % for the diffusive flux estimation.

Ammonium remineralization, calculated either by the stoichiometric oxygen-based N remineralization or measured total inorganic nitrogen flux (i.e. $NH_4^+ + NH_3 + N_2$-N $+ NO_3^-$), suggests elevated pH dramatically promoted N efflux. If we assume that aerobic N remineralization stoichiometry from phytoplanktonic organic matter is $138O_2$:16N and denitrification is partly fuelled by the diffusion of water column NO_3^- into sediment (Cornwell et al., 1999), $\sum NH_x$ flux accounted for 20–40 % of oxygen-based N remineralization in the control and 68–153 % of remineralized N in the high pH treatment. Alternatively, if nitrogen remineralization rates were evaluated from the sum of DIN flux, $\sum$ pH elevation increased ammonium flux as a proportion of total N remineralization from 22 % to 105 % for sediment at Powerline and 44 % to 87 % at Budds Landing. Both estimates reveal that high pH enhanced the proportion of ammonium release relative to the total remineralized N. However, the difference of NH_4^+ remineralization between the two estimates may result from the use of O_2 consumption rates instead of CO_2
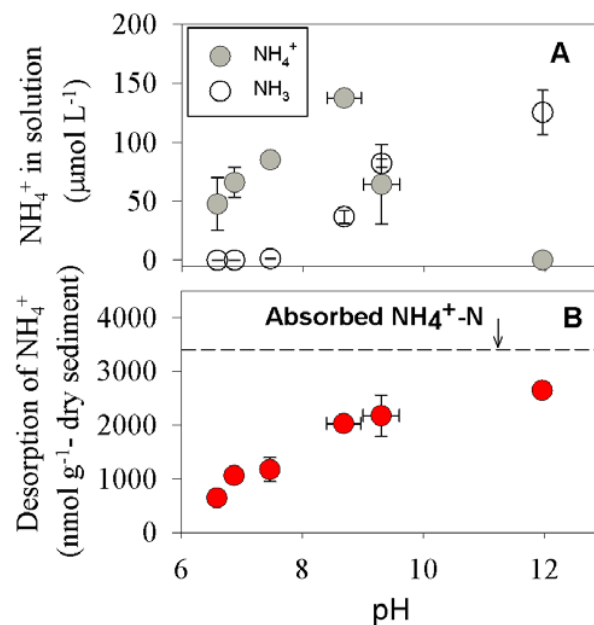

Fig. 3. Experimental pH effects on NH_4^+ concentration in solution **(A)** and desorption of exchangeable NH_4^+ **(B)**, using the 0–2 cm homogenized sediments from Budds Landing collected in November 2008. Dissolved NH_4^+ and NH_3 concentrations were estimated from the $\sum NH_x$ concentrations and pH in the aquatic phase (Eq. 2). Desorbed NH_4^+ was the sum of $\sum NH_x$ in water and the volatilized NH_3 in the headspace of the sealed centrifuge tubes (Eqs. (6), (7), and Table 3). The dashed line represents "total" absorbed NH_4^+, estimated by KCl extraction of pH-neutral sediment (Eq. 5). The vertical and horizontal error bars are the standard errors of ammonium and the pHs, respectively.

fluxes. The calculation of oxygen-based ammonium remineralization is affected by the production/reoxidation of reduced inorganic compounds (e.g. Fe^{2+}, S^{2-} and Mn^{2+}), potential methanogenesis in organic-matter rich estuaries (Martens and Klump, 1980; Carini and Joye, 2008), and variable C:N ratios of organic matter.

No significant difference was found for NO_3^- flux rates among pH treatments ($p > 0.05$, ANOVA). Fluxes of NO_3^- ranged from -70 to $10\,\mu mol\,m^{-2}\,h^{-1}$, with most fluxes
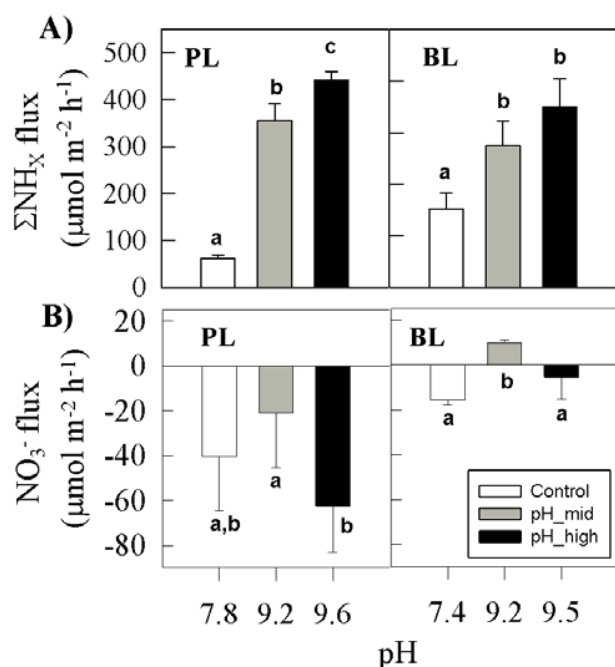
Fig. 4. Experimental pH effects on total ammonium flux rates **(A)** and nitrate flux rates **(B)**. Sediment cores were taken from Power-line (PL) and Budds Landing (BL) sites. Data are presented as mean flux rates ± standard error. At each site, different letters are used to show significant difference (Tukey's test, $P \leq 0.05$).

Fig. 5. Experimental pH effects on potential nitrification rates **(A)** and nitrification rates **(B)** from Budds Landing in July 2009. The potential nitrification rates **(A)** were calculated from nitrate production in NH_4^+-amended slurries from surficial sediments (0–2 cm). Nitrification rates **(B)** are estimated by inhibition of nitrification using CH_3F inhibitor at three pH levels of control (7.1), middle (9.1) and high (9.5). Bars show the average flux rates of $\sum NH_4^+$ (black bars) and NH_4^+ (gray bars) as well as the standard error for triplicate samples. Base on Tukey's test at the significant level of 0.05, different letters indicate significant differences in flux rates of $\sum NH_4^+$ and NH_4^+ among pHs.

directed into the sediment (Fig. 4b). In the oxygen saturated conditions, NO_2^- concentrations were generally too low to calculate flux rates via concentration changes over time.

3.9 Effect of pH on potential nitrification

The response of potential nitrification to pH suggests high pH (>9) inhibited nitrification (Fig. 5a). The potential nitrification rate in the control was 84 ± 24 nmol-N g^{-1} h^{-1}, similar to rates in other fresh water sediments of 90–470 nmol-N g^{-1} h^{-1} (Cooper, 1983). As pH was enhanced from 8 to 10, potential nitrification rates decreased sharply from above 70 nmol-N g^{-1} h^{-1} to below 10 nmol-N g^{-1} h^{-1} (Fig. 5a).

Elevated pH may have two consequences for bacterially mediated nitrification. Nitrification is considered as first order or zero-order kinetics with respect to substrates NH_4^+/NH_3 availability (Park et al., 2010). However, increases in pH can enhance $\sum NH_x$ desorption and the total inventories of exchangeable and pore water ammonium may be equal to or less than controls because of NH_3 volatilization. Moreover, high pH combined with abrupt changes in NH_3 (from zero to >550 µmol l^{-1}) may result in the physiological inhibition of nitrification. In laboratory observations and modeling, both high pH and NH_3 have negative effects on nitrifying bacteria, ammonium-oxidizing bacteria (AOB, *Nitrosomonas)* and nitrite-oxidizing bacteria (NOB, *Nitrobac-*
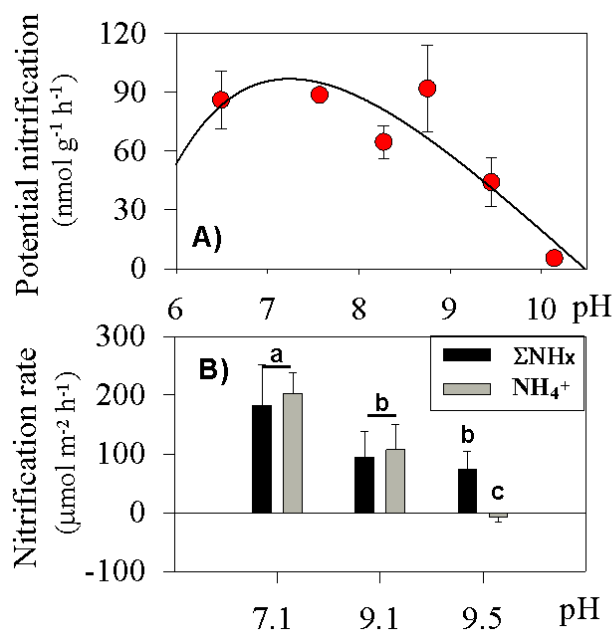
ter) (Van Hulle et al., 2007). Elevation of pH above 9 could inhibit enzyme activity of AOB and NOB since the optimal pH range is 6–8.5 for AOB and 5.5–8 for NOB (Van Hulle et al., 2007; Park et al., 2010). Even though nitrifying bacteria might survive out of the optimal pH range, they would pay an energy cost to maintain their cytoplasmic pH (Wood, 1988). The accumulation of NH_3 can be toxic or inhibit the growth and enzyme efficiency of nitrifying bacteria (Anthonisen et al., 1976; Kim et al., 2006).

Although few field studies have been conducted on the nitrification response to high pH in sediments relative to water column and soil environments (Simek et al., 2002; Carini and Joye, 2008), sediment potential nitrification rates appear to be constrained by high pH (>8) in freshwater and were positively related to exchangeable NH_4^+ in 36 stream surveys (Strauss et al., 2002). The inhibition of nitrification with elevated pH, with decreases of 80 % at pH > 9 relative to peak nitrification, has been observed in fine-grained sediment in the Arika Sea (Isnansetyo et al., 2011).

3.10 Effect of pH on nitrification rates

Elevated pH negatively impacted intact-core nitrification as measured by the changes in $\sum NH_4^+$ or NH_4^+ flux rates after adding CH_3F, an inhibitor of ammonium oxidation (Fig. 5b). Under neutral conditions, no significant difference existed between the evaluation of nitrification rates from $\sum NH_4^+$ flux ($182 \pm 49 \, \mu mol \, m^{-2} \, h^{-1}$) and from NH_4^+ flux ($210 \pm 35 \, \mu mol \, m^{-2} \, h^{-1}$). Sediments in the upper Sassafras River show considerably higher nitrification rates than the $<40 \, \mu mol \, m^{-2} \, h^{-1}$ typical observations from the mesohaline region of the Chesapeake Bay in summer (Kemp et al., 1990), reflecting the aerobic overlying water conditions.

Similar to nitrification potentials (Fig. 5a), increasing pH from neutral to 9.5 exerted a remarkable depression of nitrification rates, as evidenced by the $>50\%$ reduction in nitrification under alkaline pH levels (Fig. 5b). If both dissolved and adsorbed NH_4^+/NH_3 in sediments are assumed to be the main substrates for nitrification (Seitzinger et al., 1991), high pH increases the diffusion of $\sum NH_x$ through the oxic layer which may be lost before oxidation, lead to decreases in N availability, and functionally suppress nitrification. High pH penetration into the aerobic sediment surface (typically 1–2 mm), along with toxic NH_3 product, could suppress nitrification (Isnansetyo et al., 2011). In addition, nitrifying bacteria are obligate chemoautotrophs and grow with inorganic carbon in the form of CO_2 as their sole carbon source (Stanier et al., 1970); a reduction in CO_2 with pH elevation may therefore potentially inhibit nitrifying metabolism.

3.11 Effect of pH on denitrification

In aerobic Chesapeake Bay sediments, coupled nitrification–denitrification is the key pathway to transform the rematerialized nitrogen to N_2-N (Cornwell et al., 1999), while alternative N_2 production via annamox is inconsequential (Rich et al., 2008). Coupled nitrification–denitrification decreased from 180–280 μmol-N $m^{-2} \, h^{-1}$ to less than 85 μmol-N $m^{-2} \, h^{-1}$ as the overlying water pH increased to 9.6 (Fig. 6). Denitrification efficiency, the percentage of inorganic nitrogen released from the sediment as N_2-N (Heggie et al., 2008), decreased from 84% to 35% at Powerline and from 64% to 17% at Budds Landing.

As pH increases, reduction of denitrification may be a consequence of limited NO_3^- supply and alkaline pH inhibition of denitrifying bacterial activity. The NO_3^- supply for denitrification may come from ammonium oxidation and diffusion from the overlying water. In this study, the contribution of NO_3^- ($<7.5 \, \mu mol \, l^{-1}$) from the overlying water may be low relative to denitrification, evidenced by sediment NO_3^- uptake, accounting for $<16\%$ of denitrification, and by the undetectable NO_2^- and NO_3^- concentrations in pore water as well. As pH rises, denitrification is likely limited by the NO_3^- supply, which mostly comes from the pH-suppressed nitrification (Fig. 6).
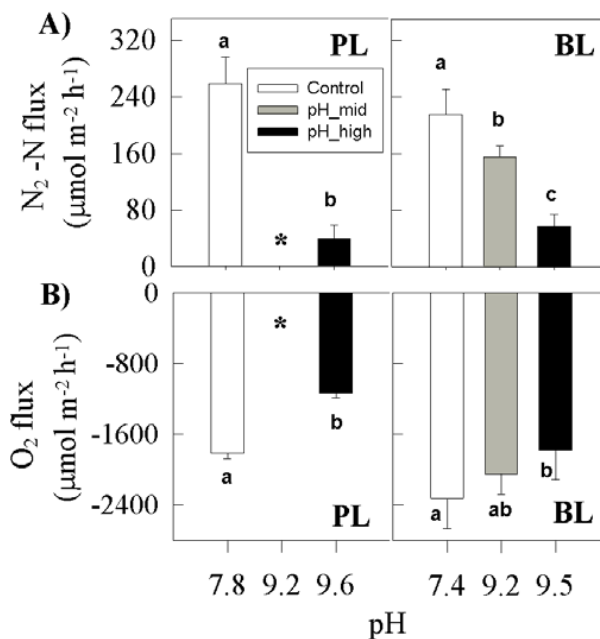

Fig. 6. Experimental pH effects on denitrification rates **(A)** and oxygen consumption rates **(B)** of sediments from the Powerline (PL) and Budds Landing (BL) sites. "*" indicates where measurements were not taken. Bars show the mean of triplicate cores, error bars are the standard error of the mean. Different letters are used to show significant difference (Tukey's test, $P \leq 0.05$) due to pH changes at PL and BL, respectively.

Moreover, the optimal pH range for denitrification is 7–8 in soil and anaerobic sediments (Simek et al., 2002); higher pH may directly inhibit the activity of denitrifying bacteria. Nitrate reducing bacteria, such as *Thioalkalivibrio nitratireducen*, can survive in alkaline sediment and cultivation media at pH 10. However, the nitrite reductase activity of *T. nitratireducens* was maximal when pH ranged from 6.7–7.5, and 80% of the activity was inhibited at high pH 9–10 (Filimonenkov et al., 2010).

Although dissimilatory nitrate reduction to ammonium (DNRA) in freshwater sediments appears to be minor relative to denitrification (Scott et al., 2008), DNRA usually occurs when NO_3^- inputs exceed the availability of carbon substrate for denitrification (Tiedje et al., 1989). As a consequence of pH elevation, limited NO_3^- consumption through anaerobic denitrification may provide the potential for DNRA and thus enhance ammonium production. Nevertheless, DNRA may play a minor role in explaining the enhanced ammonium fluxes. We did not expect high DNRA to occur in sediment with undetectable free sulfide concentrations.

3.12 Effect of pH on oxygen consumption

Oxygen consumption rates in the controls were higher in July at Budds Landing than in June at Powerline, partly a result

of increased efficiency of bacterial organic matter decomposition with rising temperatures. However, oxygen consumption decreased as pH increased at both sites (Fig. 6). This is likely related to the alkaline pH effects on bacteria production, respiration and other oxidation metabolism (Tank et al., 2009). Assuming pH has no effect on organic matter remineralization to ammonium at each sampling site, we postulate that inhibition of nitrification by increased pH resulted in the reduction of oxygen consumption.

$$NH_4^+ + 2O_2 \rightarrow NO_3^- + H_2O + 2H^+ \qquad (8)$$

The molar ratio of O_2 to $\sum NH_4^+$ is 2 for nitrification. We calculated the changes of sediment oxygen consumption and $\sum NH_4^+$ flux before and after pH treatment, respectively. The measured slopes of $\Delta \sum NH_4^+$ and $-\Delta O_2$ fluxes were consistent with nitrifying stoichiometry (Fig. 7), which suggests high pH increased sediment $\sum NH_4^+$ diffusion into overlying water rather than enhancing coupled nitrification–denitrification. Deviation of the $-\Delta O_2 : \Delta \sum NH_4^+$ flux rates from the theoretical 2:1 ratio may result from variation in sediment cores, such as oxidation of Mn (II) and Fe (II), and sediment buffering effects on OH^- penetration in depth and magnitude.

4 Conclusion and ecological implications

Although cyanobacterial blooms are increasing in frequency and magnitude over time, determining the cause of such blooms remains a challenge (Glibert et al., 2011). Cyanobacterial blooms can be locally persistent and extensive, which may cause a dramatic increase in water column pH in poorly buffered water in lakes and tidal freshwater estuaries. Nutrients, especially N, limit primary production during the extensive summer blooms in Chesapeake Bay (Kemp et al., 2005). In our study region at the Sassafras River, diazotrophic cyanobacteria are dominant bloom-forming species during N-limited summer (O'Neil and Maryland DNR, unpublished data).

Enhanced nutrient release from bottom sediments can potentially satisfy the nutrient demand by algal growth, thus enhancing eutrophic conditions. Our study suggests pH elevation can increase inorganic N supply from sediment, making it available for organismal uptake. As pH increased above 9, the DIN efflux was more than doubled by promoting NH_4^+ and NH_3 fluxes and inhibiting N_2 loss. Even though N_2-fixing cyanobacteria can survive in N deficiency, they prefer to take up dissolved inorganic N rather than consuming energy for N_2 fixation (Paerl, 2008). The pH-induced release of ammonium from sediments may thereby be an important N source for primary productivity during the blooms.

With cyanobacterial-induced pH elevation, the different modes of N and P desorption result in discrepancies in the ratio of N:P supply. The release of P may be constrained by iron oxide adsorption at the oxic surface, and can be dramatically
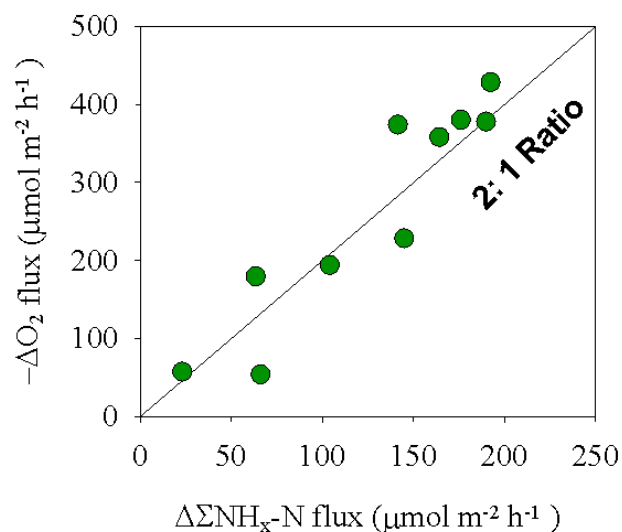

Fig. 7. The relationship between the increased $\sum NH_x$ fluxes and the reduced oxygen consumption rates after pH elevation. Data from Powerline site are the changes of $\sum NH_4^+$ and O_2 flux rates in the same core after pH was elevated from 7.8 to 9.5. Data from Budds Landing site are the changes of flux rates between control cores and cores at the pH of 9.2 and 9.5 after 7 days incubation. The slope of the solid line is 2:1, which is equal to the molar ratio of ammonium to oxygen for nitrification (Eq. 8).

increased above the threshold of pH 9–9.2 (Boers, 1991). In contrast, the corresponding desorption and release of NH_4^+ from sediment may increase more gradually in response to pH increase. The interconversion of NH_4^+–NH_3 appears to be a key to changing N efflux rates. In this study, our experimental pH levels were at or above pK_a, with only modest differences in ammonium efflux between middle pH (~ 9.2) and high pH (9.5–9.6). We hypothesize that changes in sediment N cycling at pH in the upper 8s lead to NH_3 rapidly become an important N species. The molar ratios of DIN:SRP sediment efflux decreased from >70 to 9–12 when experimental pH rose from neutral to above 9. At pH levels in the high 8s, enhanced ammonium effluxes might result in elevated N:P ratios; further investigation of pH-related changes in sediment N cycling is warranted over a broader pH range.

At our field-validated experimental pH levels, which are consistent with photosynthetic-driven pH elevation by cyanobacterial blooms, the switch of sedimentary nutrient effluxes from high N to high P may reinforce N limitation and selectively support N_2-fixing cyanobacterial blooms. Given higher P demand for diazotrophs, the augmentation of P flux with pH may boost the growth and persistence of algal blooms (Xie et al., 2003; Paerl, 2008). This, together with the increased DIN flux and diminished dentirification (N_2 loss), will lead to greater primary production and even faster element cycling in shallow waters. Cyanobacterial blooms appear to create a troublesome positive feedback that fosters

their persistence by enhancing nutrient availability from sediments.

References

Andersen, J. M.: Influence of pH on release of phosphorus from lake sediments, Archiv für Hydrobiologie, 76, 411–419, 1975.

Anthonisen, A. C., Loehr, R. C., Prakasam, T. B. S., and Srinath, E. G.: Inhibition of nitrification by ammonia and nitrous-acid, J. Water Poll. Control Fed., 48, 835–852, 1976.

Bailey, E., Owens, M., Boynton, W., and Cornwell, J.: Sediment phosphorus flux: pH interaction in the tidal freshwater Potomac River estuary, Interstate Commission on the Potomac River Basin, UMCES report TS-505-08-CBL, 1–91, 2006.

Boers, P. C. M.: The influence of pH on phosphate release from lake-sediments, Water Res., 25, 309–311, 1991.

Boudreau, B. P.: Diagenetic models and their implementation: Modeling transport and reactions in aquatic sediments, Springer, New York, 1997.

Bray, J. T., Bricker, O. P., and Troup, B. N.: Phosphate in interstitial waters of anoxic sediments – oxidation effects during sampling procedure, Science, 180, 1362–1364, 1973.

Caffrey, J. M. and Miller, L. G.: A comparison of two nitrification inhibitors used to measure nitrification rates in estuarine sediments, FEMS Microbiol. Ecol., 17, 213–220, 1995.

Cai, W. J., Luther, G. W., Cornwell, J. C., and Giblin, A. E.: Carbon cycling and the coupling between proton and electron transfer reactions in aquatic sediments in Lake Champlain, Aquat. Geochem., 16, 421–446, 2010.

Capone, D., Bronk, D., Mulholland, M., and Carpenter, E.: Nitrogen in the marine environment, edited by: Capone, D., Bronk, D., Mulholland, M., and Carpenter, E., Elsevier, Burlington, Massachusetts, 2009.

Carini, S. A. and Joye, S. B.: Nitrification in Mono Lake, California: Activity and community composition during contrasting hydrological regimes, Limnol. Oceanogr., 53, 2546–2557, 2008.

Cooper, A. B.: Population ecology of nitrifiers in a stream receiving geothermal inputs of ammonium, Appl. Environ. Microbiol., 45, 1170–1177, 1983.

Cornwell, J. and Owens, M.: Quantifying sediment nitrogen releases associated with estuarine dredging, Aquat. Geochem., 17, 499–517, 2011.

Cornwell, J. C. and Sampou, P. A.: Environmental controls on iron sulfide mineral formation in a coastal plain estuary, in: Geochemical Transformations of Sedimentary Sulfur, edited by: Vairavamurthy, M. A. and Schoonen, M. A. A., American Chemical Society, Washington, DC, 224–242, 1995.

Cornwell, J. C., Kemp, W. M., and Kana, T. M.: Denitrification in coastal ecosystems: methods, environmental controls and ecosystem level controls, a review, Aquat. Ecol., 33, 41–54, 1999.

Cowan, J. L. W. and Boynton, W. R.: Sediment-water oxygen and nutrient exchanges along the longitudinal axis of Chesapeake Bay: Seasonal patterns, controlling factors and ecological significance, Estuaries, 19, 562–580, 1996.

Cuhel, J., Simek, M., Laughlin, R. J., Bru, D., Cheneby, D., Watson, C. J., and Philippot, L.: Insights into the effect of soil pH on N_2O and N_2 emissions and denitrifier community size and activity, Appl. Environ. Microbiol., 76, 1870–1878, 2010.

Eckert, W., Nishri, A., and Parparova, R.: Factors regulating the flux of phosphate at the sediment-water interface of a subtropical calcareous lake: A simulation study with intact sediment cores, Water Air Soil Pollut., 99, 401–409, 1997.

Filimonenkov, A. A., Zvyagilskaya, R. A., Tikhonova, T. V., and Popov, V. O.: Isolation and characterization of nitrate reductase from the halophilic sulfur-oxidizing bacterium *Thioalkalivibrio nitratireducens*, Biochemistry, 75, 744–751, 2010.

Fisher, T. R., Carlson, P. R., and Barber, R. T.: Sediment nutrient regeneration in Three North Carolina estuaries, Estuar. Coast. Shelf Sci., 14, 101–116, 1982.

Folk, R.: Petrology of Sedimentary Rocks, Hemphill Publishing Company, Austin, TX, 1974.

Garcia-Ruiz, R., Pattinson, S. N., and Whitton, B. A.: Denitrification in river sediments: relationships between process rate and properties of water and sediment, Freshw. Biol., 39, 467–476, 1998.

Gardner, W. S., Seitzinger, S. P., and Malczyk, J. M.: The effects of sea salts on the forms of nitrogen released from estuarine and fresh-water sediments – Does ion-pairing affect ammonium flux, Estuaries, 14, 157–166, 1991.

Gibbs, M. M.: A simple method for the rapid determination of iron in natural waters, Water Res., 13, 295–297, 1979.

Glibert, P. M., Fullerton, D., Burkholder, J. M., Cornwell, J. C., and Kana, T. M.: Ecological stoichiometry, biogeochemical cycling, invasive species, and aquatic food webs: San Francisco estuary and comparative systems, Rev. Fish. Sci., 19, 1–60, 2011.

Hansen, P. J.: Effect of high pH on the growth and survival of marine phytoplankton: implications for species succession, Aquat. Microb. Ecol., 28, 279–288, 2002.

Heggie, D. T., Logan, G. A., Smith, C. S., Fredericks, D. J., and Palmer, D.: Biogeochemical processes at the sediment-water interface, Bombah Broadwater, Myall Lakes, Hydrobiologia, 608, 49–67, 2008.

Henriksen, K., Hansen, J. I., and Blackburn, T. H.: Rates of nitrification, distribution of nitrifying bacteria, and nitrate fluxes in different types of sediment from danish waters, Mar. Biol., 61, 299–304, 1981.

Hinga, K. R.: Effects of pH on coastal marine phytoplankton, Mar. Ecol. Prog. Ser., 238, 281–300, 2002.

Hutchins, C. M., Teasdale, P. R., Lee, J., and Simpson, S. L.: The effect of manipulating sediment pH on the porewater chemistry of copper- and zinc-spiked sediments, Chemosphere, 69, 1089–1099, 2007.

Isnansetyo, A., Thien, N. D., and Seguchi, M.: Potential of mud sediment of the Ariake Sea tidal flat and the individual effect of temperature, ph, salinity and ammonium concentration on its

nitrification rate, Res. J Environ. Earth Sci., 3, 587–599, 2011.

Kana, T. M. and Weiss, D. L.: Comment on "comparison of isotope pairing and N$_2$: Ar methods for measuring sediment denitrification" by B. D. Eyre, S. Rysgaard, T. Dalsgaard, and P. Bondo Christensen, 2002. estuaries 25: 1077–1087, Estuaries, 27, 173–176, 2004.

Kana, T. M., Darkangelo, C., Hunt, M. D., Oldham, J. B., Bennett, G. E., and Cornwell, J. C.: Membrane inlet mass spectrometer for rapid high-precision determination of N$_2$, O$_2$, and Ar in environmental water samples, Anal. Chem., 66, 4166–4170, 1994.

Kana, T. M., Cornwell, J. C., and Zhong, L. J.: Determination of denitrification in the Chesapeake Bay from measurements of N$_2$ accumulation in bottom water, Estuar. Coast., 29, 222–231, 2006.

Kemp, W. M. and Boynton, W. R.: Spatial and temporal coupling of nutrient inputs to estuarine primary production – the role of particulate transport and decomposition, Bull. Mar. Sci., 35, 522–535, 1984.

Kemp, W. M., Sampou, P., Caffrey, J., Mayer, M., Henriksen, K., and Boynton, W. R.: Ammonium recycling versus denitrification in Chesapeake Bay sediments, Limnol. Oceanogr., 35, 1545–1563, 1990.

Kemp, W. M., Boynton, W. R., Adolf, J. E., Boesch, D. F., Boicourt, W. C., Brush, G., Cornwell, J., Fisher, T., Glibert, P., Hagy, J., Harding, L., Houde, E., Kimmel, D., Miller, W., Newell, R., Roman, M., Smith, E., and Stevenson, J.: Eutrophication of Chesapeake Bay: historical trends and ecological interactions, Mar. Ecol. Prog. Ser., 303, 1–29, 2005.

Killham, K.: Soil Ecology, Cambridge University Press, Cambridge, 1994.

Kim, D. J., Lee, D. I., and Keller, J.: Effect of temperature and free ammonia on nitrification and nitrite accumulation in landfill leachate and analysis of its nitrifying bacterial community by FISH, Bioresour. Technol., 97, 459–468, 2006.

Kopp, J. F. and McKee, G. D.: Methods for Chemical Analysis of Water and Wastes, United States Environmental Protection Angency (EPA), Cincinnati, OH, 1983.

Koop, K., Boynton, W. R., Wulff, F., and Carman, R.: Sediment-water oxygen and nutrient exchanges along a depth gradient in the Baltic sea, Mar. Ecol. Prog. Ser., 63, 65–77, 1990.

Laima, M. J. C.: Extraction and seasonal variation of NH$_4^+$ pools in different types of coastal marine sediments, Mar. Ecol. Prog. Ser., 82, 75–84, 1992.

Laima, M. J. C., Girard, M. F., Vouve, F., Blanchard, G. F., Gouleau, D., Galois, R., and Richard, P.: Distribution of adsorbed ammonium pools in two intertidal sedimentary structures, Marennes-Oleron Bay, France, Mar. Ecol. Prog. Ser., 182, 29–35, 1999.

Larsen, R. K., Steinbacher, J. C., and Baker, J. E.: Ammonia exchange between the atmosphere and the surface waters at two locations in the Chesapeake Bay, Environ. Sci. Technol., 35, 4731–4738, 2001.

Mackin, J. E. and Aller, R. C.: Ammonium adsorption in marine sediments, Limnol. Oceanogr., 29, 250–257, 1984.

Magalhaes, C. M., Bordalo, A. A., and Wiebe, W. J.: Temporal and spatial patterns of intertidal sediment-water nutrient and oxygen fluxes in the Douro River estuary, Portugal, Mar. Ecol. Prog. Ser., 233, 55–71, 2002.

Martens, C. S. and Klump, J. V.: Biogeochemical cycling in an organic-rich coastal marine basin. 1. methane sediment-water exchange processes, Geochim. Cosmochim. Acta, 44, 471–490, 1980.

Martin, W. R. and Banta, G. T.: The measurement of sediment irrigation rates – a comparison of the br-tracer and ^{222}Rn/^{226}Ra disequilibrium techniques, J. Mar. Res., 50, 125–154, 1992.

Morin, J. and Morse, J. W.: Ammonium release from resuspended sediments in the Laguna Madre estuary, Mar. Chem., 65, 97–110, 1999.

Mulholland, M.: Gaseous nitrogen compounds (NO, N$_2$O, N$_2$, NH$_3$) in the ocean, in: Nitrogen in the Marine Environment, edited by: Capone, D., Mulholland, M., and Carpenter, E., Elsevier, Burlington, MA, 52–123, 2008.

Nixon, S. W., Ammerman, J. W., Atkinson, L. P., Berounsky, V. M., Billen, G., Boicourt, W. C., Boynton, W. R., Church, T. M., Ditoro, D. M., Elmgren, R., Garber, J. H., Giblin, A. E., Jahnke, R. A., Owens, N. J. P., Pilson, M. E. Q., and Seitzinger, S. P.: The fate of nitrogen and phosphorus at the land sea margin of the North Atlantic Ocean, Biogeochemistry, 35, 141–180, 1996.

Paerl, H.: Nutrient and other environmental controls of harmful cyanobacterial blooms along the freshwater-marine continuum, in: Cyanobacterial Harmful Algal Blooms: State of the Science and Research Needs, edited by: Hudnell, K., Springer, North Carolina, USA, 217–237, 2008.

Park, S., Bae, W., and Rittmann, B. E.: Operational boundaries for nitrite accumulation in nitrification based on minimum/maximum substrate concentrations that include effects of oxygen limitation, pH, and free ammonia and free nitrous acid inhibition, Environ. Sci. Technol., 44, 335–342, 2010.

Parsons, T. R., Maita, Y., and Lalli, C. M.: Fluorometric determination of chlorophylls, in: A Manual of Chemical and Biological Methods for Seawater Analysis, edited by: Parsons, T. R. and Robert Maxwell, M. C., New York, 107–108, 1984.

Price, G. D., Badger, M. R., Woodger, F. J., and Long, B. M.: Advances in understanding the cyanobacterial CO$_2$-concentrating-mechanism (CCM): functional components, Ci transporters, diversity, genetic regulation and prospects for engineering into plants, J. Exp. Bot., 59, 1441–1461, 2008.

Rao, A. M. F. and Jahnke, R. A.: Quantifying porewater exchange across the sediment-water interface in the deep sea with *in situ* tracer studies, Limnol. Oceanogr.-Method, 2, 75–90, 2004.

Rich, J. J., Dale, O. R., Song, B., and Ward, B. B.: Anaerobic ammonium oxidation (anammox) in Chesapeake Bay sediments, Microb. Ecol., 55, 311–320, 2008.

Roden, E. E. and Tuttle, J. H.: Sulfide release from estuarine sediments underlying anoxic bottom water, Limnol. Oceanogr., 37, 725–738, 1992.

Rosenfeld, J. K.: Ammonium adsorption in nearshore anoxic sediments, Limnol. Oceanogr., 24, 356–364, 1979.

Schulz, K. G., Riebesell, U., Rost, B., Thoms, S., and Zeebe, R. E.: Determination of the rate constants for the carbon dioxide to bicarbonate inter-conversion in pH-buffered seawater systems, Mar. Chem., 100, 53–65, 2006.

Scott, J. T., McCarthy, M. J., Gardner, W. S., and Doyle, R. D.: Denitrification, dissimilatory nitrate reduction to ammonium, and nitrogen fixation along a nitrate concentration gradient in a created freshwater wetland, Biogeochemistry, 87, 99–111, 2008.

Seitzinger, S.: The effect of pH on the release of phosphorus from Potomac River sediment, Cheasapeake Bay program, Report No. 86-8F, 1–46, 1987.

Seitzinger, S. P.: The effect of pH on the release of phosphorus from Potomac estuary sediments – implications for blue-green-algal blooms, Estuar. Coast. Shelf Sci., 33, 409–418, 1991.

Seitzinger, S. P., Gardner, W. S., and Spratt, A. K.: The effect of salinity on ammonium sorption in aquatic sediments – implications for benthic nutrient recycling, Estuaries, 14, 167–174, 1991.

Simek, M., Jisova, L., and Hopkins, D. W.: What is the so-called optimum pH for denitrification in soil?, Soil Biol. Biochem., 34, 1227–1234, 2002.

Simon, N. S. and Kennedy, M. M.: The distribution of nitrogen species and adsorption of ammonium in sediments from the tidal Potomac River and estuary, Estuar. Coast. Shelf Sci., 25, 11–26, 1987.

Slomp, C. P., Malschaert, J. F. P., and Van Raaphorst, W.: The role of adsorption in sediment-water exchange of phosphate in North Sea continental margin sediments, Limnol. Oceanogr., 43, 832–846, 1998.

Soetaert, K., Hofmann, A. F., Middelburg, J. J., Meysman, F. J. R., and Greenwood, J.: The effect of biogeochemical processes on pH, Mar. Chem., 106, 380–401, 2007.

Stanier, R. Y., Doudoroff, M., and Adelberg, E. A.: Other groups of gram-negative nonphotosynthetic true bacteria, in: The microbial world, 3 Edn., Prentice-Hall, Inc., NJ, 873, 1970.

Strauss, E. A., Mitchell, N. L., and Lamberti, G. A.: Factors regulating nitrification in aquatic sediments: effects of organic carbon, nitrogen availability, and pH, Can. J. Fish. Aquat. Sci., 59, 554–563, 2002.

Tango, P. J. and Butler, W.: Cyanotoxins in tidal waters of Chesapeake Bay, Northeast. Nat., 15, 403–416, 2008.

Tank, S. E., Lesack, L. F. W., and McQueen, D. J.: Elevated pH regulates bacterial carbon cycling in lakes with high photosynthetic activity, Ecology, 90, 1910–1922, 2009.

Tiedje, J. M., Simkins, S., and Groffman, P. M.: Perspectives on measurement of denitrification in the field including recommended protocols for acetylene based methods, Plant Soil, 115, 261–284, 1989.

Van Hulle, S. W. H., Volcke, E. I. P., Teruel, J. L., Donckels, B., van Loosdrecht, M. C. M., and Vanrolleghem, P. A.: Influence of temperature and pH on the kinetics of the Sharon nitritation process, J. Chem. Technol. Biotechnol., 82, 471–480, 2007.

Van Nester, A. and Duce, R. A.: Methylamines in the marine atmosphere, Geophys. Res. Lett., 14, 711–714, 1987.

Vouve, F., Guiraud, G., Marol, C., Girard, M., Richard, P., and Laima, M. J. C.: NH_4^+ turnover in intertidal sediments of Marennes-Oleron Bay (France): effect of sediment temperature, Oceanologica Acta, 23, 575–584, 2000.

Wang, F. L. and Alva, A. K.: Ammonium adsorption and desorption in sandy soils, Soil Sci. Soc. Am. J., 64, 1669–1674, 2000.

Weston, N. B., Giblin, A. E., Banta, G. T., Hopkinson, C. S., and Tucker, J.: The effects of varying salinity on ammonium exchange in estuarine sediments of the Parker River, Massachusetts, Estuar. Coast., 33, 985–1003, 2010.

Wood, P.: Monooxygenase and free radical mechanismsfor biological ammonia oxidation, in: The Nitrogen and Sulphur Cycles, edited by: Cole, J., and Ferguson, S., Cambridge University Press, Cambridge, UK, 219–243, 1988.

Xie, L. Q., Xie, P., and Tang, H. J.: Enhancement of dissolved phosphorus release from sediment to lake water by Microcystis blooms – an enclosure experiment in a hyper-eutrophic, subtropical Chinese lake, Environmental Pollution, 122, 391–399, Pii S0269-7491(02)00305-6, 2003.